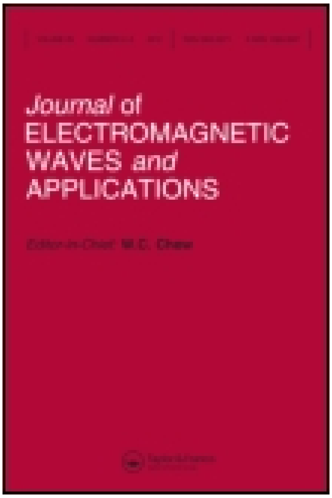


Journal of Electromagnetic Waves and Applications
Publication details, including instructions for authors and subscription information:
http://www.tandfonline.com/loi/tewa20

# An Asymmetric Arbitrary Branch-Line Coupler Terminated By One Group Of Complex Impedances

Y. L. Wu [a], J. Y. Shen [a], Q. Liu [a], L. M. Liang [a] & Y. Liu [a]
[a] School of Electronic Engineering, Beijing University of Posts and Telecommunications, Beijing, China
Published online: 25 Jul 2012.

To cite this article: Y. L. Wu, J. Y. Shen, Q. Liu, L. M. Liang & Y. Liu (2012) An Asymmetric Arbitrary Branch-Line Coupler Terminated By One Group Of Complex Impedances, Journal of Electromagnetic Waves and Applications, 26:8-9, 1125-1137, DOI: 10.1080/09205071.2012.710554

To link to this article: http://dx.doi.org/10.1080/09205071.2012.710554

*J. of Electromagn. Waves and Appl., Vol. 26, 1125–1137, 2012*

# AN ASYMMETRIC ARBITRARY BRANCH-LINE COUPLER TERMINATED BY ONE GROUP OF COMPLEX IMPEDANCES

**Y. L. Wu*, J. Y. Shen, Q. Liu, L. M. Liang, and Y. Liu**

School of Electronic Engineering, Beijing University of Posts and Telecommunications, Beijing, China



**Abstract**—A novel arbitrary asymmetric branch-line coupler structure terminated by one group of complex impedances is proposed. Two left ports of the proposed branch-line coupler are terminated by equal arbitrary complex impedances, and the other two right ports are terminated by equal real impedances. Arbitrary power division ratios are feasible for the proposed structure. Using rigorous even- and odd-mode analysis and scattering parameters theory based on complex impedances, the closed-form design formulas for designing the proposed branch-line coupler is obtained. To validate the proposed structure and the given design equations, a microstrip branch-line coupler operating at the center frequency of 2.5 GHz and terminated by 20 and $30 - 6j$ Ohm impedances is designed, simulated and measured. There is a good agreement between the simulated and measured results.

## 1. INTRODUCTION

Branch-line couplers and power dividers are essential building blocks of mobile microwave telecommunication system. More specially, both of them are widely used in power amplifiers, antenna array systems, mixers and filters. With the common points of power splitting, they have particular characteristics, respectively. Note that for output phase difference, the power divider has an in-phase output, while the branch-line coupler offers a 90° phase difference. Due to the increasing demands in passive and active circuits, the conventional Wilkinson power divider and the conventional 3-dB directional coupler [1] have limited structures to achieve high-performance required by versatile applications for mobile communication system,

*Received 10 March 2012, Accepted 9 April 2012, Scheduled 23 April 2012*
* Corresponding author: Yongle Wu (wuyongle138@gmail.com).

such as multiband, broadband, unequal power divisions, multichannel, harmonic suppression, and compactness. To this end, many researches have been devoted to novel power dividers [2–4] and branch-line couplers [5–13].

Regarding the dual-band branch-line couplers, the $\pi$-topology dual-band microstrip line was introduced to replace the conventional $\lambda/4$ transmission line [5, 6]. Note that the latter coupler realized the arbitrary power division ratios [6]. In addition, Yeung proposed a dual-band coupler with three $\lambda/4$ coupled-line sections [7]. Furthermore, tri-band branch-line couplers with three controllable operating frequencies were reported [8, 9]. With respect to bandwidth enhancement, a novel branch-line coupler using coupled port feeding was proposed [10]. To obtain a small size, the miniaturized 3-dB branch-line coupler utilized the space within the coupler to arrange the distributed capacitors [11]. Dual paralleled transmission lines were proposed to replace the conventional $\lambda/4$ transmission lines to achieve a compact structure [12]. Harmonic suppression remains another bottleneck of a high-performance coupler, and a compact slow-wave microstrip branch-line coupler using high-low impedance resonant cells periodically was reported in [13].

However, all of the reviewed approaches only consider the loads as ***real*** source and load impedances. For general microwave circuits, especially active circuits and systems, ***complex*** impedances occur frequently. Unfortunately, there is a vacuum on the field of branch-line couplers terminated by arbitrary complex impedances.

Therefore, this study proposes an asymmetric arbitrary branch-line coupler terminated by one group of complex impedances. With the ports terminated by complex impedances, the branch-line coupler serves as the impedances transformers between real and complex ones. Moreover, arbitrary power division ratios are feasible for the proposed structure. As a simple structure, this proposed coupler utilizes no stubs or more sections and is easy to fabricate. The closed-form design formulas of the proposed coupler are achieved through rigorous even- and odd-mode analysis and scattering parameters theory based on complex impedances from [14]. Experimental results are demonstrated to validate the proposed branch-line structure and the presented design theory.

## 2. CIRCUIT STRUCTURE AND DESIGN THEORY

Figure 1 depicts the schematic diagram of the proposed branch-line coupler. It is an asymmetric branch-line coupler terminated by equal complex impedances $Z_S$ $(R_S + jX_S)$ for both the **Port 1** and **Port 4**

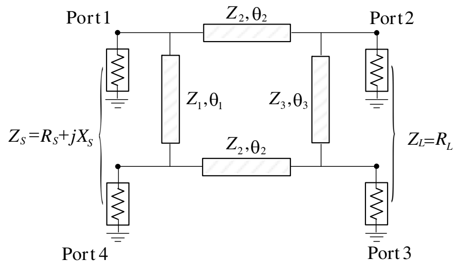


**Figure 1.** The equivalent circuit diagram of the proposed asymmetric arbitrary branch-line coupler terminated by one group of complex impedances.

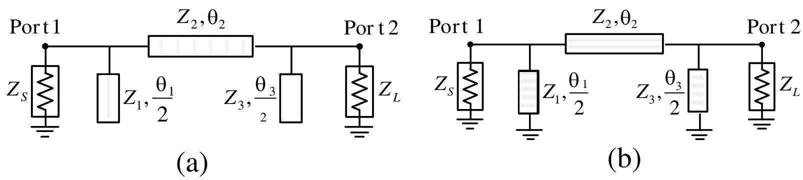


**Figure 2.** The equivalent circuit diagrams for the proposed branch-line coupler under, (a) even- and (b) odd-mode excitations.

and equal real impedances $Z_L\,(R_L)$ for both the **Port 2** and **Port 3**. Moreover, left and right branches of the proposed coupler have the characteristic impedances of $Z_1$ and $Z_3$ and electrical lengths of $\theta_1$ and $\theta_3$, respectively. Meanwhile, the characteristic impedance of lateral transmission line located at the center place in the circuit configuration of the proposed coupler is $Z_2$, and the corresponding electrical length is defined as $\theta_2$.

The proposed branch-line coupler shown in Figure 1 is symmetric along the horizontal axis, and this structure could be divided into the even- and odd-mode half circuits for simple analysis, as shown in Figures 2(a) and (b), respectively.

In the even- and odd-mode half circuits in Figures 2(a) and (b), the ABCD-parameters of the half circuits can be simply derived as [5]

$$\begin{bmatrix} A & B \\ C & D \end{bmatrix}_e = \begin{bmatrix} 1 & 0 \\ \dfrac{j\tan\left(\dfrac{\theta_1}{2}\right)}{Z_1} & 1 \end{bmatrix} \begin{bmatrix} \cos(\theta_2) & jZ_2\sin(\theta_2) \\ \dfrac{j\sin(\theta_2)}{Z_2} & \cos(\theta_2) \end{bmatrix} \begin{bmatrix} 1 & 0 \\ \dfrac{j\tan\left(\dfrac{\theta_3}{2}\right)}{Z_3} & 1 \end{bmatrix} \quad \text{(1a)}$$

$$\begin{bmatrix} A & B \\ C & D \end{bmatrix}_o = \begin{bmatrix} 1 & 0 \\ \dfrac{1}{jZ_1 \tan\left(\dfrac{\theta_1}{2}\right)} & 1 \end{bmatrix} \begin{bmatrix} \cos(\theta_2) & jZ_2 \sin(\theta_2) \\ \dfrac{j\sin(\theta_2)}{Z_2} & \cos(\theta_2) \end{bmatrix} \begin{bmatrix} 1 & 0 \\ \dfrac{1}{jZ_3 \tan\left(\dfrac{\theta_3}{2}\right)} & 1 \end{bmatrix}, \quad (1b)$$

where $e$ and $o$ represent the even- and odd- modes, respectively. After straightforward manipulation, the ABCD matrices of the even- and odd-modes half circuits can be written as

$$\begin{bmatrix} A & B \\ C & D \end{bmatrix}_e = \begin{bmatrix} \cos\theta_2 - \dfrac{Z_2 \tan\dfrac{\theta_3}{2}\sin\theta_2}{Z_3} & jZ_2\sin\theta_2 \\ \dfrac{j\tan\dfrac{\theta_1}{2}\cos\theta_2}{Z_1} + \dfrac{j\sin\theta_2}{Z_2} + \dfrac{j\tan\dfrac{\theta_3}{2}\cos\theta_2}{Z_3} - \dfrac{jZ_2\tan\dfrac{\theta_1}{2}\tan\dfrac{\theta_3}{2}\sin\theta_2}{Z_1Z_3} & \cos\theta_2 - \dfrac{Z_2\tan\dfrac{\theta_1}{2}\sin\theta_2}{Z_1} \end{bmatrix} \quad (2a)$$

$$\begin{bmatrix} A & B \\ C & D \end{bmatrix}_o = \begin{bmatrix} \cos\theta_2 + \dfrac{Z_2\sin\theta_2}{Z_3\tan\dfrac{\theta_3}{2}} & jZ_2\sin\theta_2 \\ \dfrac{\cos\theta_2}{j\tan\dfrac{\theta_1}{2}Z_1} + \dfrac{j\sin\theta_2}{Z_2} + \dfrac{\cos\theta_2}{j\tan\dfrac{\theta_3}{2}Z_3} + \dfrac{Z_2\sin\theta_2}{jZ_1Z_3\tan\dfrac{\theta_1}{2}\tan\dfrac{\theta_3}{2}} & \cos\theta_2 + \dfrac{Z_2\sin\theta_2}{\tan\dfrac{\theta_1}{2}Z_1} \end{bmatrix}. \quad (2b)$$

In view of complex terminated impedances, the reflection and transmission scattering parameters are presented in terms of ABCD parameters as [14]

$$\Gamma_e = \frac{A_eZ_L + B_e - C_eZ_S^*Z_L - D_eZ_S^*}{A_eZ_L + B_e + C_eZ_SZ_L + D_eZ_S} \quad (3a)$$

$$\Gamma_o = \frac{A_oZ_L + B_o - C_oZ_S^*Z_L - D_oZ_S^*}{A_oZ_L + B_o + C_oZ_SZ_L + D_oZ_S} \quad (3b)$$

$$T_e = \frac{2\sqrt{\mathrm{Re}(Z_S)\mathrm{Re}(Z_L)}}{A_eZ_L + B_e + C_eZ_SZ_L + D_eZ_S} \quad (3c)$$

$$T_o = \frac{2\sqrt{\mathrm{Re}(Z_S)\mathrm{Re}(Z_L)}}{A_oZ_L + B_o + C_oZ_SZ_L + D_oZ_S}, \tag{3d}$$

where $Z_S^*$ is the complex conjugate of $Z_S$. $\mathrm{Re}\,(Z_S)$ and $\mathrm{Re}\,(Z_L)$ represent the real parts of $Z_S$ and $Z_L$, respectively.

After synthesizing the reflection and transmission coefficients in even- and odd-modes half circuits, the final input and output scattering parameters of the proposed branch-line coupler are given by [14]

$$S_{11} = \frac{\Gamma_e + \Gamma_o}{2} \tag{4a}$$

$$S_{21} = \frac{T_e + T_o}{2} \tag{4b}$$

$$S_{31} = \frac{T_e - T_o}{2} \tag{4c}$$

$$S_{41} = \frac{\Gamma_e - \Gamma_o}{2}. \tag{4d}$$

For a branch-line coupler in Figure 1 with ideal matching and isolation performance, the requirements of $S_{11} = 0$ and $S_{41} = 0$ become necessary. According to these conditions, Equations (4a) and (4d) are reduced to

$$\Gamma_e = 0, \quad \Gamma_o = 0. \tag{5}$$

Moreover, the proposed branch-line coupler can divide the input signal at **Port 1** into two outputs at **Ports 2** and **3** with equal/unequal magnitude and 90° phase difference, as shown in Figure 1. This requirement leads to the following relationship between the scattering parameters $S_{21}$ and $S_{31}$ as

$$\frac{S_{31}}{S_{21}} = \mathrm{j}k, \tag{6}$$

where $k$ is the power division ratio. Eliminating $S_{21}$ and $S_{31}$ from Equations (4b), (4c) and (6) gives the following equation:

$$\frac{T_o}{T_e} = \frac{1 - \mathrm{j}k}{1 + \mathrm{j}k}. \tag{7}$$

By substituting Equation (3) into (5) and (7), we can obtain

$$A_eZ_L + B_e - C_eZ_S^*Z_L - D_eZ_S^* = 0 \tag{8a}$$

$$A_oZ_L + B_o - C_oZ_S^*Z_L - D_oZ_S^* = 0 \tag{8b}$$

$$\frac{A_eZ_L + B_e + C_eZ_SZ_L + D_eZ_S}{A_oZ_L + B_o + C_oZ_SZ_L + D_oZ_S} = \frac{1 - jk}{1 + jk}. \tag{8c}$$

As mentioned earlier, the complex terminated impedance is $Z_S = R_S + jX_S$, and real terminated impedance is purely resistive, i.e.,

$Z_L = R_L$. The real and imaginary parts of Equations 8(a)–(c) can be written, respectively, as

$$A_e R_L + jC_e X_S R_L - D_e R_S = 0 \tag{9a}$$

$$B_e - C_e R_S R_L + jD_e X_S = 0 \tag{9b}$$

$$A_o R_L + jC_o X_S R_L - D_o R_S = 0 \tag{9c}$$

$$B_o - C_o R_S R_L + jD_e X_S = 0 \tag{9d}$$

$$\begin{aligned} &A_e R_L + jC_e X_S R_L + D_e R_S + jkB_e + jkC_e R_S R_L - kD_e X_S \\ &= A_o R_L + jC_o X_S R_L + D_o R_S - jkB_o - jkC_o R_S R_L + kD_o X_S \end{aligned} \tag{9e}$$

$$\begin{aligned} &B_e + C_e R_S R_L + jD_e X_S + jkA_e R_L - kC_e X_S R_L + jkD_e R_S \\ &= B_o + C_o R_S R_L + jD_o X_S - jkA_o R_L + kC_o X_S R_L - jkD_o R_S. \end{aligned} \tag{9f}$$

Here, parameters $Z_1$, $Z_2$, $Z_3$ are solved simultaneously after substituting Equation (2) into (9). These characteristic impedances values can be calculated by

$$Z_1 = -\frac{R_S^2 + X_S^2}{kR_S \sin\theta_1}. \tag{10}$$

$$Z_2 = -\frac{R_S^2 + X_S^2}{(-kR_S \cos\theta_1 + X_S)\tan\theta_2}. \tag{11}$$

$$Z_3 = -\frac{R_L}{k\sin\theta_3}. \tag{12}$$

Meanwhile, other two equations are obtained as

$$\frac{R_S^2 + X_S^2}{kR_S \cos\theta_1 - X_S} = \frac{-R_L R_S + R_S^2 + X_S^2}{k(\cos\theta_1 - \cos\theta_3)R_S - X_S}. \tag{13}$$

$$\begin{aligned} &Z_2 \tan\theta_2 + \left(1 - \frac{Z_2 \tan\theta_2}{Z_1} \tan\frac{\theta_1}{2}\right) X_S = \\ &\left(\frac{1}{Z_1}\tan\frac{\theta_1}{2} + \frac{\tan\theta_2}{Z_2} + \frac{1}{Z_3}\tan\frac{\theta_3}{2} - \frac{Z_2 \tan\theta_2}{Z_1 Z_3}\tan\frac{\theta_1}{2}\tan\frac{\theta_3}{2}\right) R_S R_L. \end{aligned} \tag{14}$$

Solving for the two arbitrary parameters (e.g., $\theta_2$, $\theta_3$) of the $\theta_1$, $\theta_2$, $\theta_3$ (assuming $-1 \leq k < 0$), we found the closed-form solution for $\theta_3$ from Equation (13), and the result is

$$\theta_3 = \arccos\left[\frac{R_L(kR_S\cos\theta_1 - X_S)}{k\left(R_S^2 + X_S^2\right)}\right]. \tag{15}$$

Therefore, when $\theta_3$ is found, $\theta_2$ can be also calculated by, regarding $Z_1$, $Z_2$, and $Z_3$ as positive, one of the following two solutions derived from Equations (10)–(12), (14) and (15) as

$$\theta_2(1)=\arctan\left[\frac{\sqrt{\begin{array}{l}kR_LR_S(1-\cos\theta_1)(kR_S\cos\theta_1-X_S)-\\ \left(R_Sk^2\cos\theta_3-R_S-R_Sk^2-kX_S\cos\theta_3\right)\left(R_S^2+X_S^2\right)\end{array}}}{\sqrt{R_L}(kR_S\cos\theta_1-X_S)}\right], \tag{16a}$$

$$\theta_2(2)=-\theta_2(1). \tag{16b}$$

Thus, once the terminal impedances $Z_S(R_S + jX_S)$, $Z_L(R_L)$, power division ratio $k$ and the electrical length $\theta_1$ (the random parameter among $\theta_1$, $\theta_2$ and $\theta_3$) are determined, and the inequality $-1 \leq k < 0$ is satisfied, other parameters such as $\theta_2$, $\theta_3$, $Z_1$, $Z_2$, and $Z_3$ can be easily yielded according to Equations (10)–(12), (15) and (16). In consequence, the design approach of this proposed branch-line coupler is ***analytical***. Furthermore, it is necessary to investigate the input and output external performances ($S_{11}$, $S_{21}$, $S_{31}$, and $S_{41}$) of the designed coupler. In addition, the parameters can be easily obtained using the above-mentioned design equations. After substituting Equations (10)–(12), (15) and (16) into (2), we can obtain the ABCD matrices of the proposed branch-line coupler. Conversion from ABCD-parameters to scattering parameters is easy to realize through Equations (3) and (4). Finally, the input and output external scattering performances can be easily synthesized.

## 3. DESIGN EXAMPLE AND MEASUREMENT

A novel asymmetric arbitrary branch-line coupler terminated by one group of complex impedance is designed and measured by following the above analysis. Another power division ratio $m$ of direct output power (**Port 2** in Figure 1) to coupled output power (**Port 3** in Figure 1) is defined and given by

$$q = 20 * \log\left(-\frac{1}{k}\right) \quad \text{or} \quad q = 10 * \log m. \tag{17}$$

In Equation (17), $q$ has the unit of dB on the power division ratio. This equation could be reduced to the following one:

$$k = -\frac{1}{\sqrt{m}}. \tag{18}$$

We assume that the complex source impedance $Z_S = (30-6j)\,\Omega$ as the terminated impedance of port 1 and port 4 (in Figure 1), and the load

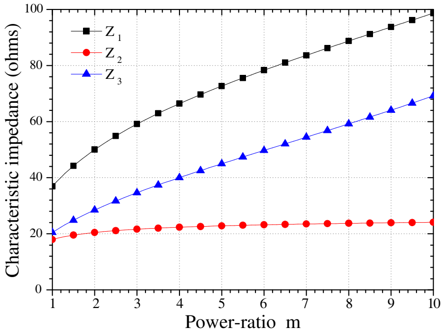


(a)

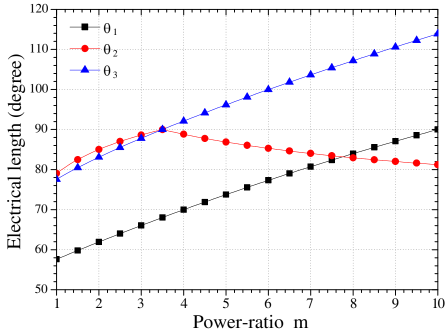


(b)

**Figure 3.** Calculated results of the proposed branch-line coupler, (a) characteristic impedances, (b) electrical lengths.

impedance $Z_L = 20\,\Omega$ as the port impedance of the port 2 and port 3 (in Figure 1). After calculation of Equations (10)–(12), (15) and (16), the electrical length $\theta_1$, which is suitable for the range of $1 < m < 10$ (the transmission lines can be implemented in microstrip technology), can be chosen manually from the following equation

$$\theta_1 = 2 * \arctan\left[\frac{1}{2}\left(1 + \frac{m}{10}\right)\right]. \tag{19}$$

The characteristic impedances and electrical lengths of four branches for the proposed branch-line coupler are calculated with the varying power division ratio $m$ ($1 < m < 10$) and plotted in Figure 3. The numerical results in this plot are derived from Equations (10)–(12), (15), (16) and (19). In this case, the value of $\theta_1$ is ***manually*** defined. It can be observed from the Figure 3(a) that the characteristic impedances $Z_1$, $Z_2$, and $Z_3$ increase with the increasing power division ratio $m$. The impedance ranges of these three transmission line are $36.9\,\Omega$ to $98.7\,\Omega$, $18.0\,\Omega$ to $24.1\,\Omega$, and $20.5\,\Omega$ to $69.2\,\Omega$, respectively, which are available in microstrip technology by a double-sided printed circuit board (PCB). Figure 3(b) shows that $\theta_2$ has a peak value caused by the feature of function arctan $[f(k)]$ in the frequency range in Equation (16) and the positive requirement of $\theta_2$.

To satisfy the convenience of the application, the value of power division ratio $m$ can be flexibly chosen. The frequency responses of the proposed branch-line coupler are calculated for two specific power division ratios $m = 1$ and $m = 4$, and the corresponding simulated results are presented in Figures 4 and 5, respectively. The center frequency is $f = 2.5\,\text{GHz}$ in calculations.

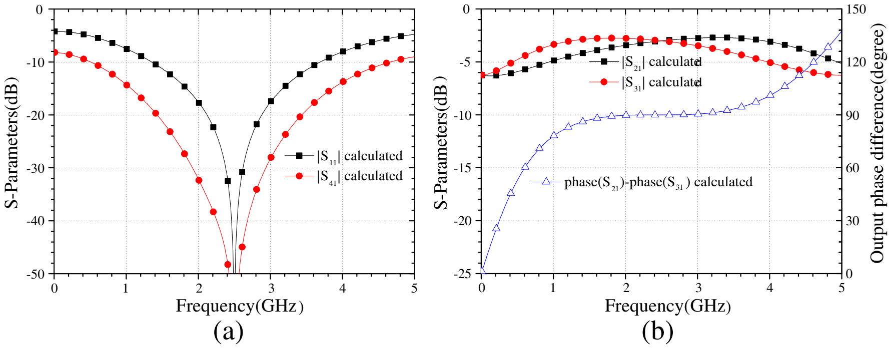


**Figure 4.** The input and output performance of the proposed branch-line coupler operating at $f = 2.5\,\text{GHz}$ with a power division ratio $m = 1$, (a) ideal input matching and output isolation parameters, (b) ideal output transmission parameters and out phase difference.

The input matching ($|S_{11}|$) and output isolation ($|S_{41}|$) characteristics in Figure 4(a) and Figure 5(a) meet the requirements of below $-20\,\text{dB}$ at the center frequency. The output transmission characteristics in Figure 4(b) and Figure 5(b) indicate that the direct output ($|S_{21}|$) and coupled output ($|S_{31}|$) have the same power and 6 dB power difference, respectively, and both have 90° phase difference at the center frequency $f = 2.5\,\text{GHz}$. On the other hand, the frequency response for $m = 1$ in Figure 4 shows better performance in terms of bandwidth and quadrature output phase difference than the case $m = 4$ shown in Figure 5.

A prototype of branch-line coupler has been designed, fabricated, and measured based on the analyses presented above. The power division ratio is chosen as $m = 8$ at the center frequency $f = 2.5\,\text{GHz}$. The electrical lengths of the branches of this proposed branch-line coupler are calculated as $\theta_1 = 84.0°$, $\theta_2 = 82.9°$, $\theta_3 = 107.2°$ according to Equations (15), (16) and (19). Synthesized from Equations (10)–(12), other parameters are $Z_1 = 88.7\,\Omega$, $Z_2 = 23.7\,\Omega$ and $Z_3 = 59.2\,\Omega$. Since the standard microwave adapter impedance is $50\,\Omega$, four additional sections of transmission lines are designed between the adapters and original complex or real ports as impedance transformers. This designed branch-line coupler is fabricated using the microstrip transmission lines on a Rogers4350B substrate with a dielectric constant of 3.48 and a thickness of 0.85 mm. Figures 6(a) and (b) show the circuit layout and photograph of the fabricated microstrip branch-line coupler, respectively. The measured results are obtained from an Agilent N5230C Vector Network Analyzer. All the

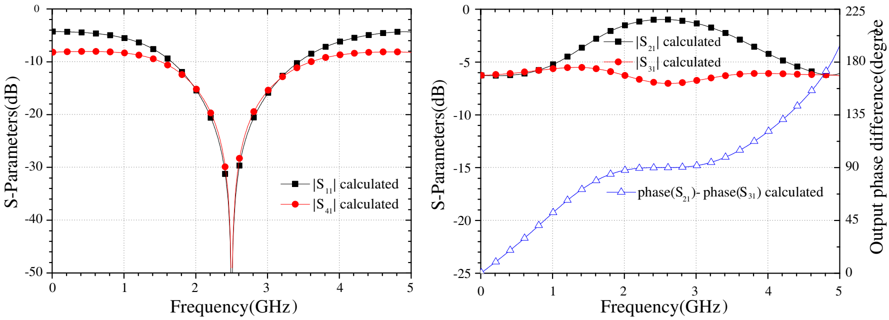


(a) (b)

**Figure 5.** The input and output performance of the proposed branch-line coupler operating at $f = 2.5$ GHz with a power divided ratio of $m = 4$, (a) ideal input matching and output isolation parameters. (b) Ideal output transmission parameters and out phase difference.

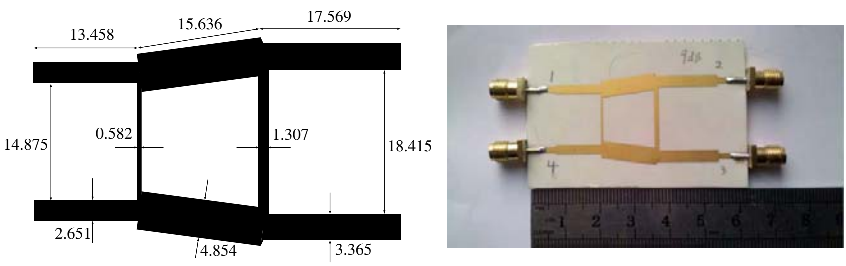


(a) (b)

**Figure 6.** (a) Circuit layout (unit: millimeters). (b) Photograph of the fabricated microstrip branch-line coupler operating at 2.5 GHz.

EM simulated results are obtained by HFSS. The frequency responses of the fabricated branch-line coupler are shown in Figure 7.

A reasonable agreement can be observed by comparing the EM simulated results (Based on the HFSS software tool) and measured results in Figure 7. The measured results show that the input matching is $-41.5$ dB, and the output isolation is $-23.3$ dB at the defined center frequency $f = 2.5$ GHz, indicating that there is a good return loss and high isolation, as displayed in the Figure 7(a). The measured insertion loss values for Port 2 and Port 3 are $-0.78$ dB (the EM simulated value is $-0.71$ dB) and $-9.54$ dB (the EM simulated value is $-8.92$ dB) at the center frequency in Figure 7(b), approximating designed 9 dB power difference. The measured 90° phase difference between the direct output and coupled output is located in a wide frequency range of

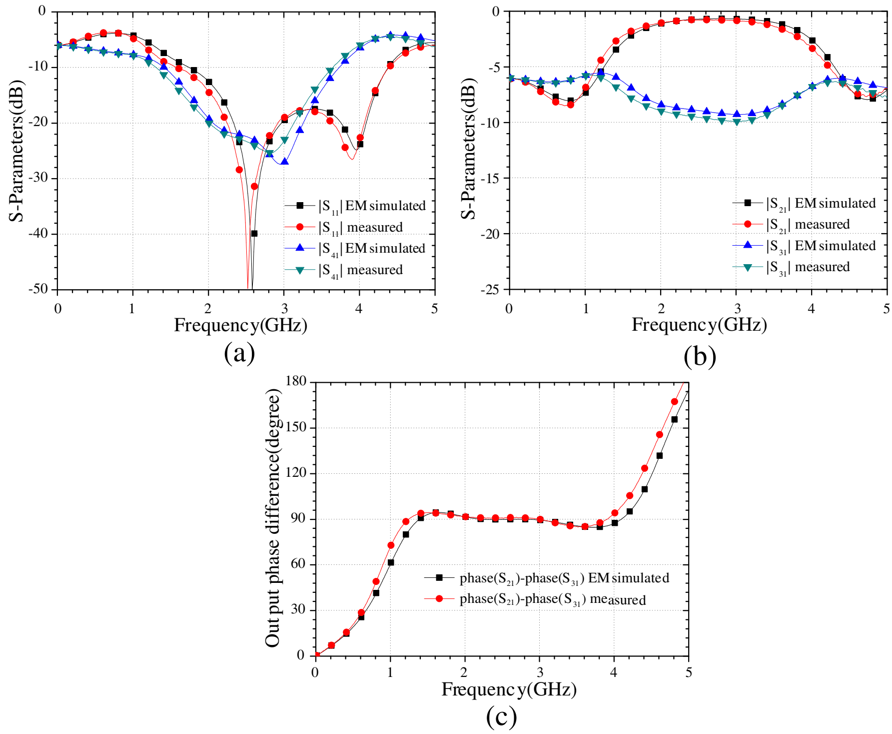


**Figure 7.** The EM simulated and measured input and output performance of the fabricated branch-line coupler shown in Figure 6. (a) Input matching and output isolation. (b) Output transmission. (c) Out phase difference.

almost 2 GHz with the center frequency $f = 2.5$ GHz. Between the EM simulated and measured results, there are some discrepancies whatever in input and output performances. The junction discontinuities are regarded as the main factor of that.

## 4. CONCLUSIONS

An asymmetric arbitrary branch-line coupler terminated by one group of complex impedances is proposed. The closed-form design formulas are given through rigorous even- and odd-mode analysis and scattering parameters theory based on complex terminated impedances. The proposed branch-line coupler is easy to design and fabricate. It is believed that the proposed branch-line coupler with complex terminated impedances can be used widely in designing Doherty amplifiers and antenna arrays, in particular, active sub systems with complex source or load impedances.

## ACKNOWLEDGMENT

This work was supported in part by the Fundamental Research Funds for the Central Universities (No. 2012RC0301), National Natural Science Foundation of China (No. 61001060), and Important National Science & Technology Specific Projects (No. 2010ZX03007-003-04).



## REFERENCES

1. Reed, J. and G. Wheeler, "A method of analysis of symmetrical four-port networks," *IRE Trans. on Microw. Theory and Tech.*, Vol. 4, No. 10, 246–252, 1956.
2. Deng, P.-H., J.-H. Guo, and W.-C. Kuo, "New wilkinson power dividers based on compact stepped-impedance transmission lines and shunt open stubs," *Progress In Electromagnetics Research*, Vol. 123, 407–426, 2012.
3. Al-Zayed, A. S. and S. F. Mahmoud, "Seven ports power divider with various power division ratios," *Progress In Electromagnetics Research*, Vol. 114, 383–393, 2011.
4. Wu, Y. and Y. Liu, "An unequal coupled-line wilkinson power divider for arbitrary terminated impedances," *Progress In Electromagnetics Research*, Vol. 117, 181–194, 2011.
5. Cheng, K.-K. and F.-L. Wong, "A novel approach to the design and implementation of dual-band compact planar 90° branch-line coupler," *IEEE Trans. on Microw. Theory and Tech.*, Vol. 52, No. 11, 2458–2463, 2004.
6. Hsu, C. L., J. T. Kuo, and C. W. Chang, "Miniaturized dual-band hybrid couplers with arbitrary power division ratios," *IEEE Trans. on Microw. Theory and Tech.*, Vol. 57, No. 1, 149–156, 2009.
7. Yeung, L. K., "A compact dual-band 90° coupler with coupled-line sections," *IEEE Trans. on Microw. Theory and Tech.*, Vol. 50, No. 9, 2227–2232, 2011
8. Lin, F., Q.-X. Chu, and Z. Lin, "A novel tri-band branch-line coupler with three controllable operating frequencies," *IEEE Microw. Wireless Compon. Lett.*, Vol. 20, No. 12, 666–668, 2010.
9. Liou, C.-Y., M.-S. Wu, J.-C. Yeh, Y.-Z. Chueh, and S.-G. Mao, "A novel triple-band microstrip branch-line coupler with arbitrary

operating frequencies," *IEEE Microw. Wireless Compon. Lett.*, Vol. 19, No. 11, 683–685, 2009.

10. Wong, Y. S., S. Y. Zheng, and W. S. Chan, "Multifolded bandwidth branch line coupler with filtering characteristic using coupled port feeding," *Progress In Electromagnetics Research*, Vol. 118, 17–35, 2011.
11. Jung, S. C., R. Negra, and F. M. Ghannouchi, "A design methodology for miniaturized 3-dB branch-line hybrid couplers using distributed capacitors printed in the inner area," *IEEE Trans. on Microw. Theory and Tech.*, Vol. 56, No. 12, 2950–2953, 2008.
12. Tang, C. W., M. G. Chen, and C. H. Tsai, "Miniaturization of microstrip branch-line coupler with dual transmission lines," *IEEE Microw. Wireless Compon. Lett.*, Vol. 18, No. 3, 185–187, 2008.
13. Wang, J. P., B. Z. Wang, Y. X. Guo, L. C. Ong, and S. Q. Xiao, "A compact slow-wave microstrip branch-line coupler with high performance," *IEEE Microw. Wireless Compon. Lett.*, Vol. 17, No. 7, 501–503, 2007.
14. Ahn, H.-R. and B. Kim, "Toward integrated circuit size reduction," *IEEE Microw. Mag.*, Vol. 9, No. 1, 65–75, 2008.